Journal of Nuclear Medicine, published on May 8, 2020 as doi:10.2967/jnumed.119.238998

Receptor-targeted photodynamic therapy of glucagon-like peptide 1 receptor positive lesions

Marti Boss, Desiree Bos, Cathelijne Frielink, Gerwin Sandker, Patricia Bronkhorst, Sanne A.M. van Lith, Maarten Brom, Mijke Buitinga, Martin Gotthardt

Department of Radiology and Nuclear Medicine, Radboud University Medical Center, Nijmegen, The Netherlands

Running title: PDT of GLP-1R positive lesions

Corresponding author:

Marti Boss, PhD student

Geert Grooteplein-Zuid 10, P.O. Box 9101, 6500 HB, Nijmegen

+31243613813

marti.boss@radboudumc.nl

Contact Marti Boss for reprint requests

Disclosures:

This work is supported by BetaCure (FP7/2014–2018, grant agreement 602812). Martin G declares that he is an inventor and holder of the patent “Invention affecting GLP-1 and exendin” (Philips-Universität Marburg, June 17, 2009). All other authors declare that they have no conflicts of interest.

Word count: 4931

ABSTRACT

Treatment of hyperinsulinemic hypoglycemia is challenging. Surgical treatment of insulinomas and focal lesions in congenital hyperinsulinism (CHI) is invasive and carries major risks of morbidity. Medication to treat nesidioblastosis and diffuse CHI has varying efficacy and causes significant side effects. Here, we describe a novel method for therapy of hyperinsulinemic hyperglycemia, highly selectively killing beta cells by receptor-targeted photodynamic therapy (rtPDT) with exendin-4-IRDye700DX, targeting the glucagon-like peptide 1 receptor (GLP-1R).

A competitive binding assay was performed using Chinese hamster lung (CHL) cells transfected with the GLP-1R. The efficacy and specificity of rtPDT with exendin-4-IRDye700DX was examined *in vitro* in cells with different levels of GLP-1R expression. Tracer biodistribution was determined in BALB/c nude mice bearing subcutaneous CHL-GLP-1R xenografts. Induction of cellular damage and the effect on tumor growth were analyzed to determine treatment efficacy.

Exendin-4-IRDye700DX has a high affinity for the GLP-1R with an IC_{50} value of 6.3 nM. rtPDT caused significant specific phototoxicity in GLP-1R positive cells (2.3 ± 0.8 % and 2.7 ± 0.3 % remaining cell viability in CHL-GLP-1R and INS-1 cells resp.). The tracer accumulates dose-dependently in GLP-1R positive tumors. In vivo rtPDT induces cellular damage in tumors, shown by strong expression of cleaved-caspase-3 and leads to a prolonged median survival of the mice (36.5 vs. 22.5 days resp. $p<0.05$).

These data show *in vitro* as well as *in vivo* evidence for the potency of rtPDT using exendin-4-IRDye700DX. This could in the future provide a new, minimally invasive and highly specific treatment method for hyperinsulinemic hypoglycemia.

Keywords: glucagon-like peptide 1 receptor, exendin, photodynamic therapy, hyperinsulinemic hypoglycemia

INTRODUCTION

Insulin production by pancreatic beta cells is usually a well-regulated process. However, uncontrolled overproduction of insulin can arise, in most cases as a result of insulin-producing lesions. Such lesions cause major clinical symptoms and treatment can be challenging. In adults, these lesions manifest in endogenous adult hyperinsulinemic hypoglycemia, most often caused by an insulinoma, an insulin-producing neuroendrocrine tumor arising from pancreatic beta cells (*1*). In 0.5% to 5% of cases, adult hyperinsulinemic hypoglycemia is caused by nesidioblastosis, characterized by proliferation of abnormal beta cells throughout the pancreas (*2*). In neonates, the most common cause of persistent hyperinsulinism is CHI (*3*). In diffuse CHI, there is diffuse involvement of the pancreatic beta cells, while in focal CHI the disease is caused by focal adenomatous islet cell hyperplasia (*4*). Episodic hypoglycemia due to endogenous hyperinsulinism causes neuroglycopenic and autonomic symptoms. Prolonged hypoglycemia may lead to seizures, loss of consciousness, permanent brain damage or brain death (*5*).

Insulinomas and focal CHI can be cured by surgical removal of the lesion (*3,6*). Enucleation is possible in case of superficially localized lesions with sufficient distance to the pancreatic duct (2-3 mm). Otherwise, a more extensive surgical procedure like partial or distal pancreatectomy may be required. While such procedures can often be performed laparoscopically (*7,8*), they remain challenging and may carry major risks of morbidity (*9,10*). The only surgical treatment option for patients with nesidioblastosis and diffuse CHI not responding to medication is partial pancreatectomy. Even after such an invasive procedure, hypoglycemic episodes often persist, requiring continued treatment with medication and, in certain cases of CHI, total pancreatectomy (*2,4*).

Because of these challenges, a novel, preferably minimally invasive treatment option for hyperinsulinemic hypoglycemia in adults as well as in children is warranted. In this study, we assess the feasibility of specific ablation of insulin-producing cells with PDT. PDT is based on inducing cell death by irradiation of a light-sensitive molecule, or photosensitizer (PS). The PS

absorbs photons and is transferred to a higher energy state. By transfer of energy from the activated PS to the oxygen in the surrounding tissue, reactive oxygen species (ROS) are produced, which can cause cellular damage (*11*). To ensure efficient and specific delivery of the PS to the target tissue, the PS is coupled to a tumor-specific targeting moiety (*12*).

An attractive targeting moiety for rtPDT of insulin-producing cells is exendin-4. This peptide is a stable analogue of the hormone GLP-1. It specifically binds to the GLP-1R, which is expressed on pancreatic beta cells and in high levels in nearly 100% of benign insulinomas (*13*). GLP-1R imaging using ^{111}In- and ^{68}Ga-labelled exendin-4 has been shown to be a successful pre-operative imaging technique for insulinomas (*14-16*) and is also under investigation in CHI (clinicaltrials.gov; NCT03768518).

We have developed an approach for rtPDT of insulin producing lesions using the peptide exendin-4 coupled to the photosensitizer IRDye700DX. We hypothesize that this novel method will allow specific cell killing of GLP-1R positive cells.

MATERIALS AND METHODS

Reagents

Exendin-4-IRDye700DX was supplied by piCHEM (Graz, Austria). IRDye700DX NHS ester was obtained from LI-COR Biosciences (Lincoln, Nebraska, U.S.A.). IRDye700DX absorbs and emits light in the NIR range and has a higher extinction coefficient (2.1×10^5 $M^{-1}cm^{-1}$ at 689 nm) than non-NIR PSs (*12,17*). The N-epsilon amino group of lysine at position 40 was site specifically modified during solid phase peptide synthesis with a mercapto-propionic acid, releasing an unprotected exendin-4 with a free thiol function after triisopropylsilane cleavage. IRDye700DX was modified with a maleimide and coupling to exendin-4 was performed using a thiol reactive crosslinking approach. The purity was >90%. Stock solutions of exendin-4-IRDye700DX were prepared in phosphate-buffered saline (PBS). The structure and amino acid sequence of the tracer are shown

in supplemental figure 1. Absorbance and emission spectra of exendin-4-IRDye700DX are shown in supplemental figure 2.

Cell culture

CHL cells stably transfected with the GLP-1R (*18*) were cultured in Dulbecco's modified Eagle's medium (DMEM) with 4.5g/L D-glucose and Glutamax, supplemented with 10% fetal calf serum (FCS), 100 IU/mL penicillin G, 10mg/mL streptomycine, 1 mM sodium pyruvate, 0.1 mM non-essential amino acids and 0.3 mg/mL G418 geneticin. The rat insulinoma cell line INS-1 was cultured in RPMI 1640 medium, supplemented with 10% FCS, 100 IU/mL penicillin G, 10mg/mL streptomycine, 2 mmol/L L-glutamine, 1 mmol/L pyruvate, 10 mmol/L 4-(2-hydroxyethyl)-1-piperazineethanesulfonic acid (HEPES) and 50 µmol/L 2-mercaptoethanol. The human pancreatic tumor cell line PANC-1 was cultured in RPMI 1640 medium supplemented with 10% FCS, 100 IU/mL penicillin G, 10 mg/mL streptomycine and 2 mmol/L L-glutamine.

Competitive binding assay

The half-maximal inhibitory concentration (IC_{50}) of exendin-4-IRDye700DX and unlabeled exendin, as a reference, was determined using CHL-GLP-1R cells as described previously (*19,20*). 10^6 cells/well were grown overnight in six well plates. Cells were washed twice with PBS and incubated for 4 hours on ice with 50.000 cpm ^{111}In-labelled exendin in the presence of increasing concentrations of exendin-4-IRDye700DX (0.1–300 nM). Cells were then washed with PBS, solubilized with 2 mL sodium hydroxide (NaOH), collected and the cell-associated activity was measured in a gamma-counter (Wizard 2480, PerkinElmer, Groningen, The Netherlands).

In vitro receptor-targeted photodynamic therapy

CHL-GLP-1R cells, INS-1 cells and PANC-1 cells were seeded into 24-well plates (Thermo Scientific) (150,000 cells/well) and grown overnight. Medium was replaced by binding buffer (medium with 0.1% bovine serum albumin (w/v) (BSA)) with exendin-4-IRDye700DX (300nM for CHL-GLP-1R cells and 400nM for INS-1 and PANC-1 cells (concentrations based on optimization experiments). As a control, cells incubated with binding buffer only were used. Separate wells

were incubated with an excess (15 μM for CHL-GLP-1R cells and 20 μM for INS-1 and PANC-1 cells) of unlabeled exendin-4 together with exendin-4-IRDye700DX. After incubation at 37ºC (CHL-GLP-1R cells 4 hours, INS-1 and PANC-1 cells 24 hours), cells were washed with binding buffer. Subsequently, cells were irradiated with a NIR light-emitting diode (LED) (*21*) (emission wavelength 670-710 nm, forward voltage: 2.6 V, power output: 490 mW) using 126 individual LED bulbs ensuring homogenous illumination (*21*). CHL-GLP-1R cells were irradiated at 90 J/cm^2 (over 6 min). INS-1 and PANC-1 cells were irradiated at 150 J/cm^2 (over 10 min). Cells incubated with exendin-4-IRDye700DX that were not irradiated were included as a control. All experiments were carried out in triplicate.

Four hours after irradiation, during which the cells were kept at 37ºC and 5% CO_2, the ATP content as a measure of cell viability was determined using a CellTiter-Glo® luminescent assay (Promega Benelux, Leiden, The Netherlands) according to the instructions of the manufacturer. Luminescence was measured using a TECAN infinite M200 Pro plate reader (PerkinElmer, Groningen, The Netherlands). The ATP content as a measure of cell viability was expressed as a percentage, determined by comparing the luminescent signal with the signal from untreated cells, which were considered 100% viable.

Additionally, a co-culture of INS-1 and PANC-1 cells was plated in 24-well plates (70,000 and 40,000 cells/well, respectively). Before seeding, INS-1 cells were labeled with the fluorescent dye DiO and PANC-1 cells with DiD dye according to the manufacturer's protocol (Life Technologies, Thermo Fisher Scientific, Waltam, MA, USA). Cells were grown overnight and then incubated with 400 nM exendin-4-IRDye700DX in binding buffer or binding buffer alone for 24 hours at 37ºC and 5% CO_2. Subsequently, cells were irradiated with 150 J/cm^2 of NIR light. After four hours, cells were incubated with 1 μg/mL propidium iodide (Thermo Fisher Scientific, Waltham, MA, USA) in PBS for 15 minutes at room temperature. Cells were visualized using an EVOS microscope (Thermo Fisher Scientific, Waltam, MA, USA).

Animal tumor model

Female BALB/c nude mice (Janvier, Le Genest Saint Isle, France), 6-8 weeks old, were housed in individually ventilated cages (6 mice per cage) under non sterile conditions with ad libitum access to chlorophyll-free animal chow and water. CHL-GLP-1R cells ($5*10^6$ cells/ mouse in 200 µl DMEM with 4.5g/L D-glucose and Glutamax) were injected subcutaneously on the right flank of the mice.

In vivo biodistribution

Female BALB/c nude mice with CHL-GLP-1R xenografts were injected intravenously with exendin-4-IRDye700DX in 200 µl PBS with 0.5% BSA (N=5 per group, 1, 3 and 10 µg exendin-4-IRDye-700DX). Four mice were injected with only PBS with 0.5% BSA. After 4 hours, mice were sacrificed by CO_2 asphyxiation and the tumor and organs were removed and collected in Roche MagNA Lyser tubes (F Hoffmann-La Roche Ltd., Basel, Switzerland). Radioimmunoprecipitation assay (RIPA) lysis buffer (500 µL; 50mM (hydroxymethyl)aminomethane-hydrochloride (TRIS-HCl), pH7.4 with 150 mM sodiumchloride (NaCl), 1 mM ethylenediaminetetraacetic acid (EDTA), 1% Triton-X-100 and 1% sodium dodecyl sulfate (SDS)) was added to each tube. Organs were homogenized using a Roche MagNA Lyser (F Hoffmann-La Roche Ltd., Basel, Switzerland) with repeated cycles of 6000 rpm for 25 sec with cooling on ice for 1 minute between cycles. Organ homogenates of the control mice (injected only with PBS with 0.5% BSA) were used to create standard curves of exendin-4-IRDye700DX for each organ. 100 µl of homogenates were transferred in triplicate to a black flat-bottom 96-well plate and fluorescence intensity was measured using a TECAN infinite M200 Pro plate reader (PerkinElmer, Groningen, The Netherlands) (excitation wavelength: 620 nm, emission wavelength: 700 nm). Standard curves and tracer uptake were calculated using Microsoft Office Excel 2007.

Receptor-targeted photodynamic therapy in vivo; immunohistochemistry

Female BALB/c nude mice with subcutaneous GLP-1R positive xenografts (N=8 per group) were injected intravenously with 30 µg exendin-4-IRDye700DX in 200 µl PBS with 0.5% BSA or 200 µl PBS with 0.5% BSA only, and after 4 hours exposed to 100 J/cm^2 NIR LED light. One group was

treated only with exendin-4-IRDye700DX without NIR light exposure. 2 or 24 hours after NIR light exposure, mice were sacrificed by CO_2 asphyxiation. Tumors were harvested, fixated in 4% buffered formalin, embedded in paraffin and sectioned at 4 µm thickness. Slices were deparaffinized with xylene and rehydrated in ethanol. Antigen retrieval was performed with 10 mM citrate pH 6.0 in a PT-Module (Thermo Fisher Scientific, Waltam, MA, USA) (10 min, 96ºC). Endogenous peroxidase activity was quenched with 3% H_2O_2 for 10 min. Slices were incubated with 20% normal goat serum for 30 min and subsequently with rabbit-anti-cleaved-caspase-3 (1:4000 in PBS + 1% BSA, ASP175, Cell Signaling Technology, Leiden, The Netherlands) in a humidified chamber at 4ºC overnight in the dark. Slides were then washed 3 times with 10 mM PBS and incubated with goat-anti-rabbit-biotin (1:200 in PBS + 1% BSA, Vector Laboratories, Peterborough, UK) for 30 min at room temperature. After washing with PBS, slides were incubated with Vectastain Elite ABC kit (Vector Laboratories, Peterborough, UK) for 30 min at room temperature. The bound antibodies were visualized using diaminobenzine (DAB, Bright DAB, BS04 Immunologic, VWR, Dublin, Ireland). Slides were counterstained with 3 times diluted hematoxylin (Klinipath, Olen, Belgium) for 5 seconds and mounted with a cover slip (permount, Fisher Scientific, Waltam, MA, USA).

The immunohistochemical staining was independently analyzed by two blinded observers. Scores were allocated to each slide following an ordinal 6-point scale ranging from 0 (no staining), 1 (very weak staining), 2 (weak staining), 3 (intermediate staining), 4 (intense staining) to 5 (very intense staining). The scores of the two observers were averaged.

Receptor-targeted photodynamic therapy in vivo; survival

Female BALC/c nude mice with CHL-GLP-1R xenografts were randomized into 2 groups of 8 animals based on tumor size. When tumors were at least 30 mm^3, mice were injected intravenously with 30 µg exendin-4-IRDye700DX in 200 µl PBS with 0.5% BSA or PBS with 0.5% BSA only. After 4 hours, mice were exposed to 150 J/cm^2 of NIR LED light under inhalation anesthesia (2,5% isoflurane mixed with 100% O_2 (1 L/min)). Kidneys were protected from

exposure by covering them with gauze and aluminum foil. Tumor diameters were measured by a blinded observer three times per week in three dimensions using a caliper. Mice were euthanized by CO_2 asphyxiation when tumor volume reached more than 1000 mm^3 (tumor volume was calculated by 1.25*π* (((length + width + height) / 6) ^3)). Overall survival was defined as the day that tumors reached a size of 1000 mm^3.

Statistics

Statistical calculations were performed using GraphPad Prism (GraphPad Software, La Jolla, CA, USA). IC_{50} values were calculated by fitting the data with non-linear regression using least squares fit with GraphPad Prism. *In vitro* cell viability after various treatments, assessed by a CellTiter-Glo® assay, were compared by two-way ANOVA with post-hoc Bonferroni tests. Tracer uptake in various tumors was compared between the different injected doses by one-way ANOVA.

Survival curves were compared with the log-rank (Mantel-Cox) test using GraphPad Prism (version 5.03).

Study approval

All animal experiments have been approved by the institutional Animal Welfare Committee of the Radboud University Medical Centre and were conducted in accordance to the guidelines of the Revised Dutch Act on Animal Experimentation.

RESULTS

Exendin-4-IRDye700DX binds the GLP-1R with high affinity

The IC_{50} values of exendin-4 and exendin-4-IRDye700DX, were 2.54 nM (95% CI; 1.32–4.90) and 6.25 nM (95% CI; 3.07–12.74), respectively (Fig. 1). While the binding affinity of the labeled peptide is significantly lower compared to the unlabeled peptide ($p < 0.0001$), it binds with a high affinity to the GLP-1R in the nanomolar range.

In vitro receptor-targeted PDT with exendin-4-IRDye700DX and NIR light causes specific GLP-1R positive cell death.

rtPDT with exendin-4-IRDye700DX caused significant phototoxicity in cells with high GLP-1R expression (CHL-GLP-1R cells) and the rat insulinoma cell line INS-1 cells, with GLP-1R expression comparable to human insulinomas. Remaining cell viabilities were 2.3±0.8 % and 2.7±0.3 % respectively (Fig. 2). In PANC-1 cells no cellular phototoxicity was observed under these conditions (96.1±1.2 % viable cells). Co-incubation with an excess of unlabeled exendin-4 abolished the phototoxic effect in CHL-GLP-1R cells as well as in INS-1 cells (99.3±1.3 and 98.4±2.1 % cell viability respectively). NIR light irradiation alone did not cause cellular phototoxicity in any of the cell types (106.6±1.2 %, 102.5±5.9 % and 102.0±1.8 % viable cells in CHL-GLP-1R, INS-1 and PANC-1 cells, respectively). No dark toxicity of the tracer was observed (103.3±6.7 %, 105.2±4.7 % and 103.6±1.4 % cell viability without irradiation in CHL-GLP-1R, INS-1 and PANC-1 cells, respectively). Incubation of a co-culture of INS-1 and PANC-1 cells with exendin-4-IRDye700DX followed by irradiation specifically caused cell death in INS-1 cells, as shown by co-localization of the red and green nuclei (Fig. 3). Absence of p.i. signal upon rtPDT indicated that exendin-4-IRDye700DX alone or NIR light alone did not cause cell death in either cell type.

Exendin-4-IRDye700DX accumulates in GLP-1R positive tumors.

Relative uptake of exendin-4-IRDye700DX in subcutaneous GLP-1R tumors in mice was 3.9±1.9 % injected dose (ID)/g for 1 µg tracer dose and diminishes slightly to 3.3±0.6 %ID/g for 3 µg tracer dose and 2.5±0.8 %ID/g for 10 µg tracer dose ($p = 0.25$) (Fig. 4). As a result, the absolute tumor uptake increases with increasing injected tracer doses to 25.0 µg/g with 10 µg tracer injection. Highest uptake of exendin-4-IRDye700 was observed in the kidneys, due to renal clearance.

In vivo receptor-targeted PDT causes cell death in GLP-1R positive tumors and improves survival

Analysis of the immunohistochemical staining revealed a low expression of cleaved-caspase-3 in the control groups. In both treatment groups the expression of cleaved-caspase-3 was higher than in the control groups. While the intensity of cleaved-caspase-3 staining was variable at 2 hours after treatment, the intensity of the staining was high and uniform in the tumors 24 hours after

treatment, showing a significant induction of apoptosis in the tumors. The expression of cleaved-caspase-3 was slightly increased in control group receiving only NIR light irradiation, showing that the light itself induces some cell death, most likely due to the heat produced by the LED light source (Fig. 5).

At the start of the survival experiment, sizes of the subcutaneous GLP-1R were very variable, although mean tumor sizes were similar between the groups (161±205 mm^3 (35-657 mm^3) in the exendin-4-IRDye700DX group and 171±144 mm^3 (36-480 mm^3) in the control group. Upon light exposure, tumor growth was slower in the group which received exendin-4-IRDye700DX leading to a significantly longer median survival in this group compared to the control group (36.5 vs. 22.5 days resp. $p<0.05$) (Fig. 6).

DISCUSSION

Treatment of hyperinsulinemic hypoglycemia is challenging. To address this issue, a treatment strategy which specifically destroys GLP-1R positive cells with rtPDT was developed as an alternative treatment option for all forms of hyperinsulinemic hypoglycemia.

We show effectivity of rtPDT with exendin-4-IRDye700DX *in vitro* and *in vivo*. The specific cytotoxic effect demonstrates that rtPDT with exendin-4-IRDye700DX could enable destruction of GLP-1R positive lesions without causing damage to the surrounding pancreatic tissue.

This is the first evidence of the effectiveness of a peptide-based agent for rtPDT *in vivo* to date. In the current development of tracers for rtPDT, the most widely used carrier molecules are mAbs and nanoparticles, because of their slow clearance from the circulation and high uptake in target organs. A single previous study examining rtPDT using various targeting peptides was limited to *in vitro* studies and showed no efficient cytotoxic effect (*22*).

We believe that rtPDT with exendin-4-IRDye700DX has the potential to be used as a minimally invasive technique to destroy insulin-producing cells with minimal morbidity. Upon delivery of the tracer, NIR light can be administered interstitially using diffuser fibers which are

placed into the target tissue. Using this method of so-called interstitial PDT (iPDT), it is feasible to deliver light to deeply seeded lesions/tissues. Successful results of iPDT have been obtained in for example prostate cancer (*23*), head and neck cancer (*24*) and importantly pancreatic tumors (*25*). An optimal treatment result depends on optimization of the number of light sources as well as their specific placement and power output (*26-28*). With percutaneous delivery, areas up to 23 cm^2 can be treated (*29*), making it suitable for treatment of CHI and nesidioblastosis. Alternatively, the less invasive endoscopic delivery of a fiber can be applied for treatment of small lesions, since a single fiber can be applied using this technique (*30,31*).

The data in this paper do not show 100% cell killing. Since these experiments were performed in an immunocompromised mouse model, they did not take into account the possible added effect on cell killing of the immune response elicited by PDT, as has been shown for other tumor types (*32*). Additionally, because of the minimal invasiveness of PDT, treatment can easily be repeated if hypoglycemia persist. Of interest, in a clinical situation, killing of enough cells to prevent overproduction of insulin will be sufficient, eliminating the need for 100% cell killing.

The receptor-targeted approach of PDT with exendin-4-IRDye700DX enables specific killing of GLP-1R expressing cells without damaging the surrounding tissue, and the focused irradiation of the tissue of interest avoids a risk of damaging the kidneys. Since treatment of nesidioblastosis and diffuse CHI will involve irradiation of a larger part of the pancreas, this risks development of impaired glucose tolerance. However, rtPDT has advantages over near-total pancreatectomy, since it avoids the risk of exocrine pancreatic insufficiency and is much less invasive. Also, localization and quantification of the insulin-overproducing cells based on pre-operative PET images using radiolabeled exendin-4 could be used for planning of the rtPDT to optimize the treatment and minimize side effects.

We believe that the data presented here, together with the advances in the technology of interstitial PDT, can provide a basis towards clinical translation of rtPDT using exendin-4-IRDye700DX. For this, verification of efficient targeting to human tissues as well as the potential

treatment efficacy by ex-vivo analysis of human tissues will be necessary before initiation of a first clinical trial.

CONCLUSION

Here, we show the feasibility of rtPDT with exendin-4-IRDye700DX, which is also the first demonstration of efficient PDT using small molecules *in vivo*. In the future, ablating insulin-producing cells using rtPDT with exendin-4-IRDye700DX could provide a new, minimally invasive treatment method for patients with hyperinsulinemic hypoglycemia. Since this treatment could be applied to a specific site of the pancreas in the case of insulinomas or focal CHI or to a larger pancreatic area in the case of nesidioblastosis or diffuse CHI, it clearly has the potential to be effective to normalize blood glucose regulation in all forms of hyperinsulinemic hypoglycemia.

ACKNOWLEDGEMENTS

We thank Bianca Lemmers-van de Weem, Kitty Lemmens-Hermans, Iris Lamers-Elemans, Karin de Haas-Cremers and Mike Peters for their technical assistance in the animal experiments.

AUTHOR CONTRIBUTIONS

M. Boss, S. van Lith, M. Buitinga, M. Brom and M. Gotthardt designed the study. M. Boss, D. Bos, C. Frielink, G. Sandker and P. Bronkhorst conducted the experiments. M. Boss, D. Bos and C. Frielink collected and analyzed the data. All authors discussed the results and implications and commented on the manuscript at all stages. M. Gotthardt is the guarantor of this work and, as such, had full access to all the data in the study and takes responsibility for the integrity of the data and the accuracy of the data analysis.

KEY POINTS

Question:

Does rtPDT with exendin-4-IRDye700DX enable effective and specific cell killing of GLP-1R positive cells?

Pertinent findings:

rtPDT with exendin-4-IRDye700DX causes specific phototoxicity in GLP-1R positive cells. The tracer accumulates in GLP-1R positive tumors and in vivo rtPDT causes cellular toxicity resulting in slower tumor growth.

Implications for patient care:

rtPDT with exendin-4-IRDye700DX could provide a new, minimally invasive treatment method for patients with hyperinsulinemic hypoglycemia.

REFERENCES

1. Kinova MK. Diagnostics and treatment of insulinoma. *Neoplasma.* 2015;62:692-704.

2. Witteles RM, Straus IF, Sugg SL, Koka MR, Costa EA, Kaplan EL. Adult-onset nesidioblastosis causing hypoglycemia: an important clinical entity and continuing treatment dilemma. *Arch Surg.* 2001;136:656-663.

3. Senniappan S, Shanti B, James C, Hussain K. Hyperinsulinaemic hypoglycaemia: genetic mechanisms, diagnosis and management. *J Inherit Metab Dis.* 2012;35:589-601.

4. Lord K, Dzata E, Snider KE, Gallagher PR, De Leon DD. Clinical presentation and management of children with diffuse and focal hyperinsulinism: a review of 223 cases. *J Clin Endocrinol Metab.* 2013;98:E1786-1789.

5. Iglesias P, Diez JJ. Management of endocrine disease: a clinical update on tumor-induced hypoglycemia. *Eur J Endocrinol.* 2014;170:R147-157.

6. Okabayashi T, Shima Y, Sumiyoshi T, et al. Diagnosis and management of insulinoma. *World J Gastroenterol.* 2013;19:829-837.

7. Drymousis P, Raptis DA, Spalding D, et al. Laparoscopic versus open pancreas resection for pancreatic neuroendocrine tumours: a systematic review and meta-analysis. *HPB (Oxford).* 2014;16:397-406.

8. Fernandez-Cruz L, Blanco L, Cosa R, Rendon H. Is laparoscopic resection adequate in patients with neuroendocrine pancreatic tumors? *World J Surg.* 2008;32:904-917.

9. Kowalewski AM, Szylberg L, Kasperska A, Marszalek A. The diagnosis and management of congenital and adult-onset hyperinsulinism (nesidioblastosis) - literature review. *Pol J Pathol.* 2017;68:97-101.

10. Richards ML, Gauger PG, Thompson NW, Kloos RG, Giordano TJ. Pitfalls in the surgical treatment of insulinoma. *Surgery.* 2002;132:1040-1049; discussion 1049.

11. Dolmans DE, Fukumura D, Jain RK. Photodynamic therapy for cancer. *Nat Rev Cancer.* 2003;3:380-387.

12. Mitsunaga M, Ogawa M, Kosaka N, Rosenblum LT, Choyke PL, Kobayashi H. Cancer cell-selective in vivo near infrared photoimmunotherapy targeting specific membrane molecules. *Nat Med.* 2011;17:1685-1691.

13. Reubi JC, Waser B. Concomitant expression of several peptide receptors in neuroendocrine tumours: molecular basis for in vivo multireceptor tumour targeting. *Eur J Nucl Med Mol Imaging.* 2003;30:781-793.

14. Christ E, Wild D, Ederer S, et al. Glucagon-like peptide-1 receptor imaging for the localisation of insulinomas: a prospective multicentre imaging study. *Lancet Diabetes Endocrinol.* 2013;1:115-122.

15. Christ E, Wild D, Forrer F, et al. Glucagon-like peptide-1 receptor imaging for localization of insulinomas. *J Clin Endocrinol Metab.* 2009;94:4398-4405.

16. Wild D, Macke H, Christ E, Gloor B, Reubi JC. Glucagon-like peptide 1-receptor scans to localize occult insulinomas. *N Engl J Med.* 2008;359:766-768.

17. Detty MR, Gibson SL, Wagner SJ. Current clinical and preclinical photosensitizers for use in photodynamic therapy. *J Med Chem.* 2004;47:3897-3915.

18. van Eyll B, Lankat-Buttgereit B, Bode HP, Goke R, Goke B. Signal transduction of the GLP-1-receptor cloned from a human insulinoma. *FEBS Lett.* 1994;348:7-13.

19. Brom M, Joosten L, Oyen WJ, Gotthardt M, Boerman OC. Radiolabelled GLP-1 analogues for in vivo targeting of insulinomas. *Contrast Media Mol Imaging.* 2012;7:160-166.

20. Jodal A, Lankat-Buttgereit B, Brom M, Schibli R, Behe M. A comparison of three (67/68)Ga-labelled exendin-4 derivatives for beta-cell imaging on the GLP-1 receptor: the influence of the conjugation site of NODAGA as chelator. *EJNMMI Res.* 2014;4:31.

21. de Boer E, Warram JM, Hartmans E, et al. A standardized light-emitting diode device for photoimmunotherapy. *J Nucl Med.* 2014;55:1893-1898.

22. You H, Yoon HE, Jeong PH, Ko H, Yoon JH, Kim YC. Pheophorbide-a conjugates with cancer-targeting moieties for targeted photodynamic cancer therapy. *Bioorg Med Chem.* 2015;23:1453-1462.

23. Trachtenberg J, Weersink RA, Davidson SR, et al. Vascular-targeted photodynamic therapy (padoporfin, WST09) for recurrent prostate cancer after failure of external beam radiotherapy: a study of escalating light doses. *BJU Int.* 2008;102:556-562.

24. Lou PJ, Jager HR, Jones L, Theodossy T, Bown SG, Hopper C. Interstitial photodynamic therapy as salvage treatment for recurrent head and neck cancer. *Br J Cancer.* 2004;91:441-446.

25. Bown SG, Rogowska AZ, Whitelaw DE, et al. Photodynamic therapy for cancer of the pancreas. *Gut.* 2002;50:549-557.

26. Kim MM, Darafsheh A. Light Sources and Dosimetry Techniques for Photodynamic Therapy. *Photochem Photobiol.* 2020.

27. van Doeveren TEM, Bouwmans R, Wassenaar NPM, et al. On the Development of a Light Dosimetry Planning Tool for Photodynamic Therapy in Arbitrary Shaped Cavities: Initial Results. *Photochem Photobiol.* 2020.

28. Dupont C, Baert G, Mordon S, Vermandel M. Parallelized Monte-Carlo dosimetry using graphics processing units to model cylindrical diffusers used in photodynamic therapy: From implementation to validation. *Photodiagnosis Photodyn Ther.* 2019;26:351-360.

29. Huggett MT, Jermyn M, Gillams A, et al. Phase I/II study of verteporfin photodynamic therapy in locally advanced pancreatic cancer. *Br J Cancer.* 2014;110:1698-1704.

30. DeWitt JM, Sandrasegaran K, O'Neil B, et al. Phase 1 study of EUS-guided photodynamic therapy for locally advanced pancreatic cancer. *Gastrointest Endosc.* 2019;89:390-398.

31. Choi JH, Oh D, Lee JH, et al. Initial human experience of endoscopic ultrasound-guided photodynamic therapy with a novel photosensitizer and a flexible laser-light catheter. *Endoscopy.* 2015;47:1035-1038.

32. Beltran Hernandez I, Yu Y, Ossendorp F, Korbelik M, Oliveira S. Preclinical and Clinical Evidence of Immune Responses Triggered in Oncologic Photodynamic Therapy: Clinical Recommendations. *J Clin Med.* 2020;9.

Figures

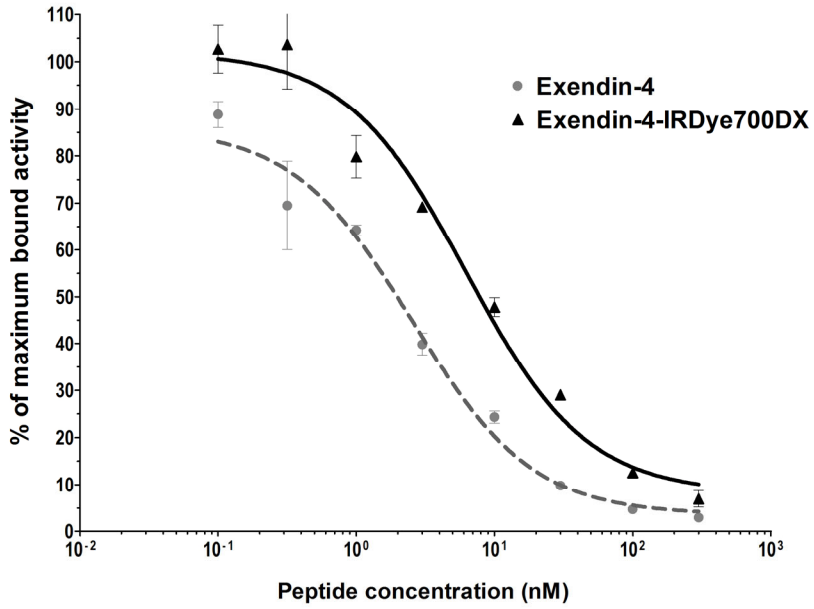

Figure 1. Competition binding assay (IC_{50}) using CHL-GLP-1 cells of unlabeled exendin-4 and exendin-4-IRDye700DX. ^{111}In-DTPA-exendin-4 was used as a tracer.

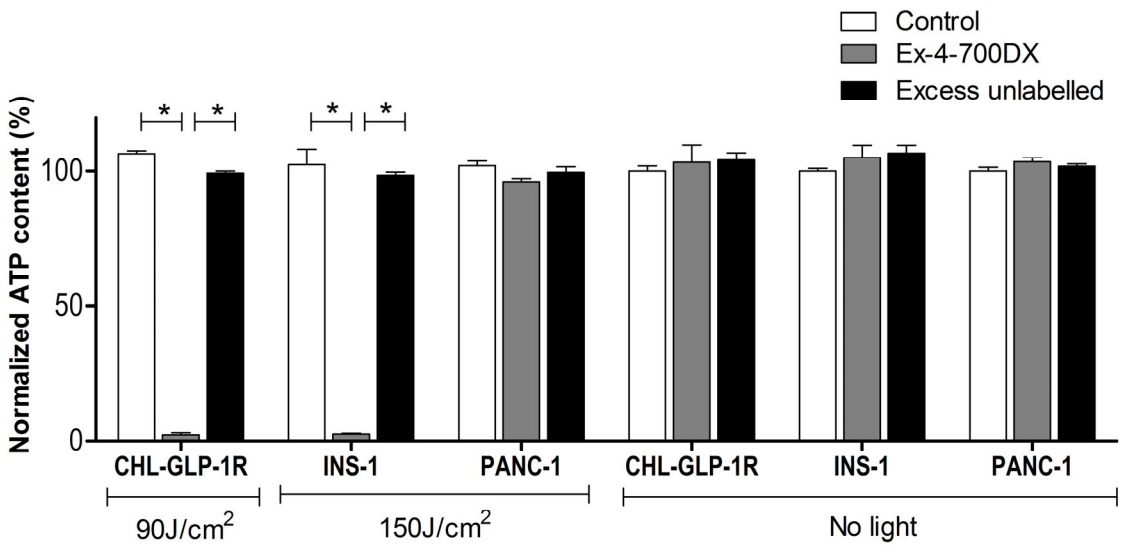

415

416 **Figure 2.** ATP content as a measure of cell viability of CHL-GLP-1R cells, INS-1 cells and PANC-1 cells
417 following incubation with binding buffer (control), exendin-4-IRDye700DX or exendin-4-IRDye-700DX
418 combined with an excess of unlabeled exendin-4 and with or without NIR light irradiation. Experiments were
419 performed in triplicate Data are presented as mean ± SD. * indicates $p<0.001$.

420

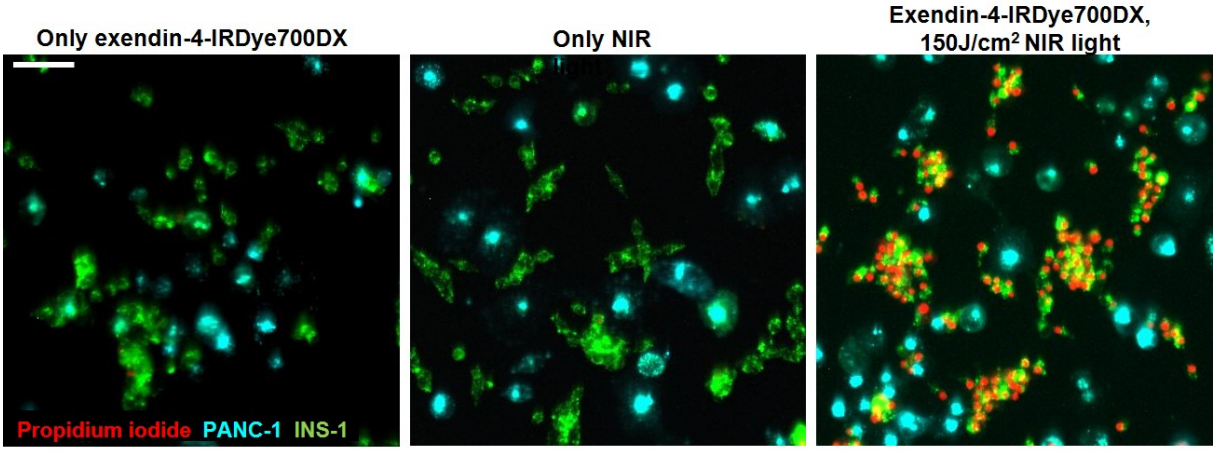

Figure 3. Fluorescence microscopy of INS-1 cells labeled with the fluorescent dye DiO (green) and PANC-1 cells labeled with the fluorescent dye DiD (cyan), co-cultured and incubated with propidium iodide (red), after incubation of exendin-4-IRDye700DX or only binding buffer and with and without NIR irradiation with a radiant exposure of 150 J/cm^2. The scale bar denotes 100 µm.

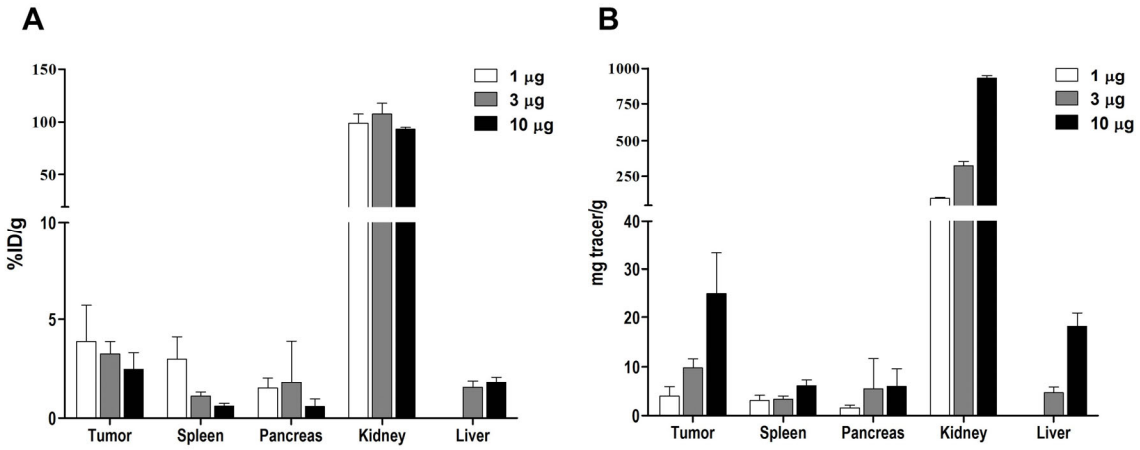

Figure 4. Biodistribution of exendin-4-IRDye700DX (1 µg, 3 µg and 10 µg, N=5 mice per group) in tumors, spleen, pancreas, kidneys and liver of female BALB/c nude mice 4 hours after tracer injection. (A) Relative uptake expressed as % of the injected dose per gram of tissue. (B) Absolute uptake expressed as µg of exendin-4-IRDye700DX per gram of tissue.

433

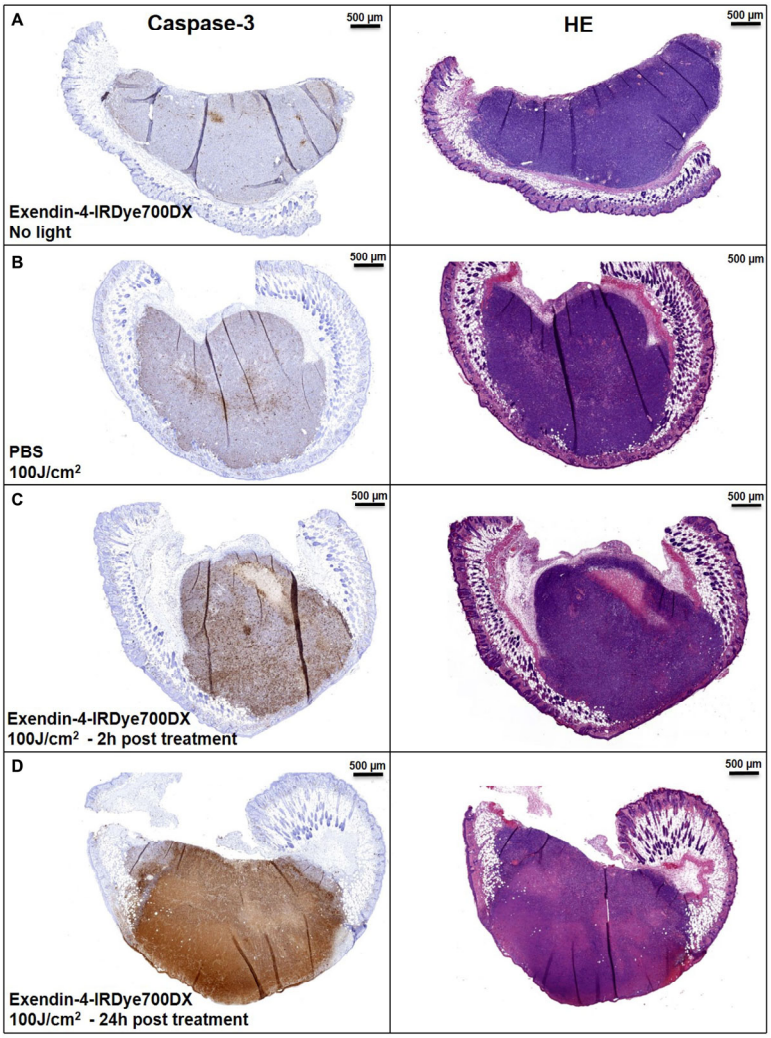

Figure 5: Representative examples of cleaved-caspase-3 and HE staining of CHL-GLP-1R tumors. A) Control tumors after i.v. administration of exendin-4-IRDye700DX. B) Control tumors after only illumination. C) Tumors after i.v. administration of exendin-4-IRDye700DX and illumination, dissected after 2 hours. D) Tumors after i.v. administration of exendin-4-IRDye700DX and illumination dissected after 24 hours. E) Intensity scores of capase-3 staining for tumor sections of all mice.

E

Intensity of the staining
0 = no staining
1 = very weak staining
2 = weak staining
3 = intermediate staining
4 = intense staining
5 = very intense staining

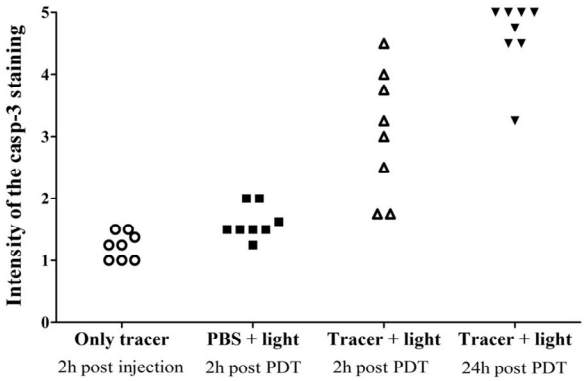

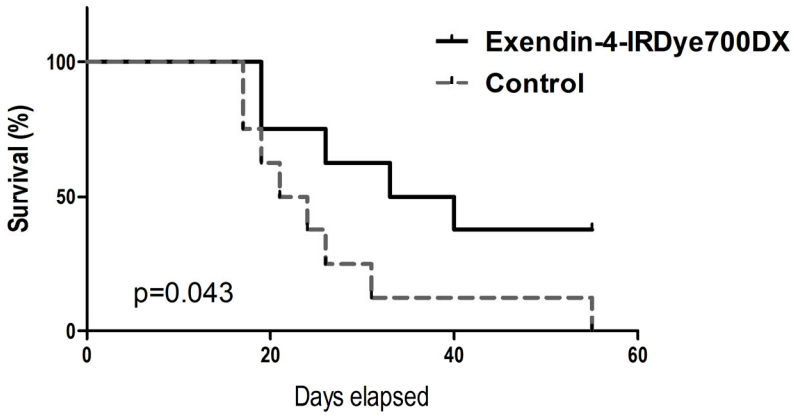

448

449

450 **Figure 6.** Kaplan-Meier plot of survival of BALB/c nude mice with GLP-1R positive tumors after injection of
451 30 µg exendin-4-IRDye700DX or PBS (control), followed by illuminaton with a radiant exposure of 150
452 J/cm^2.

Supplementary data

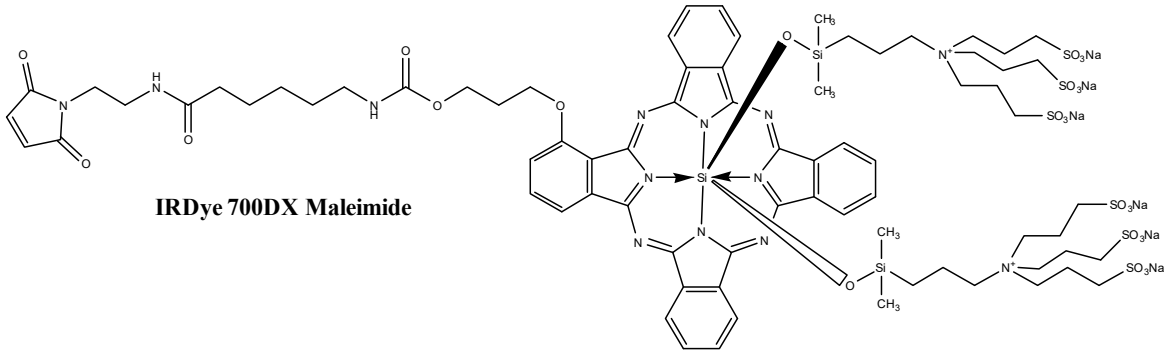

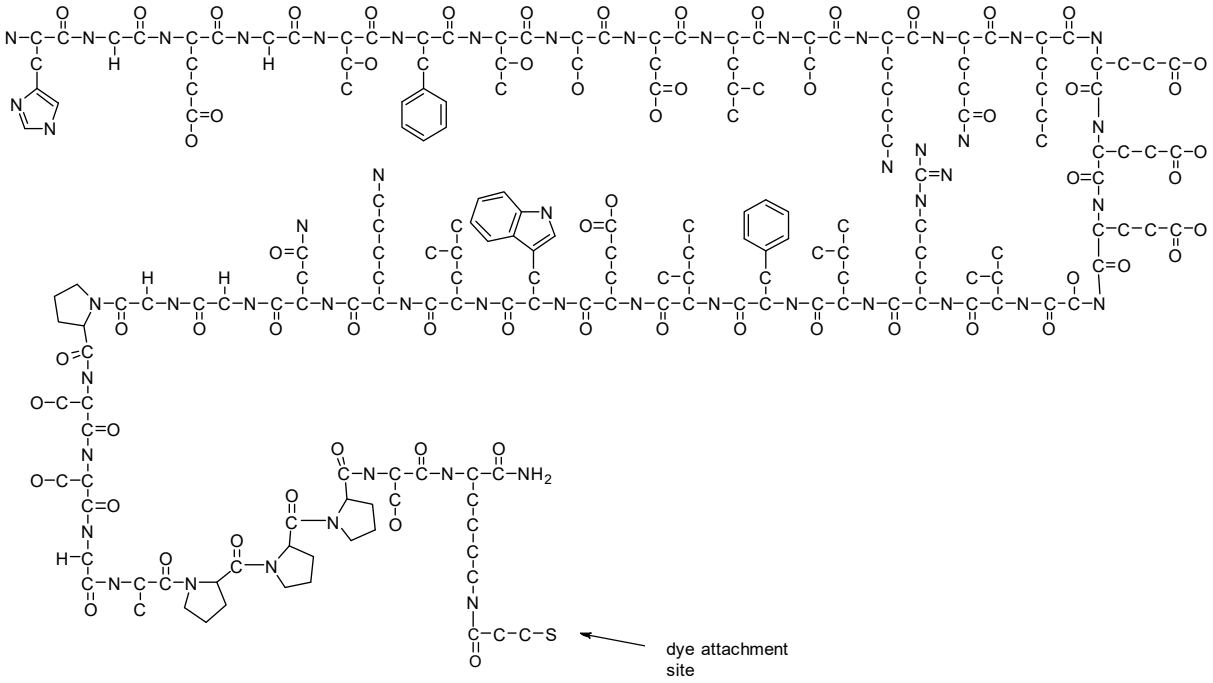

Product: Nle14-Lys40(Mep)-Exendin-4 AE4
His-Gly-Glu-Gly-Thr-Phe-Thr-Ser-Asp-Leu-Ser-Lys-Gln-Nle-Glu-Glu-Glu-Ala-Val-Arg-Leu-Phe-Ile-Glu-Trp-Leu-Lys-Asn-Gly-Gly-Pro-Ser-Ser-Gly-Ala-Pro-Pro-Pro-Ser-Lys (Mep)-NH2

Molecular Weight: 4386,87

Supplemental Figure 1: Structure and amino acid sequence of exendin-4-IRDye700DX

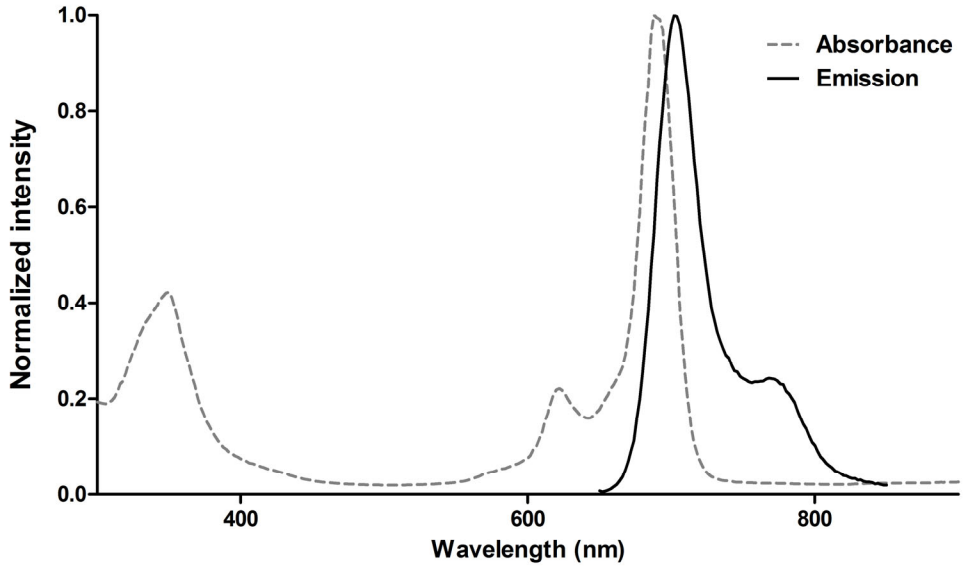

Supplemental Figure 2: Absorbance and emission spectra of exendin-4-IRDye700DX